Drying of *Matricaria recutita* Flowers in Vibrofluidized Bed Dryer: Optimization of Drying Conditions Using Response Surface Methodology

Zamani, Sahar; Rahimi, Mahmood Reza*+

Processes Intensification Research Lab, Department of Chemical Engineering, Faculty of Engineering, Yasouj University, P.O. Box 75918-74831 Yasouj, I.R. IRAN

Sadeghi, Hossein

Medicinal Plants Research Center, Yasuj University of Medical Sciences, P.O. Box 75917-41417 Yasuj, I.R. IRAN

ABSTRACT: *Drying of Matricaria recutita flower was investigated experimentally in a VibroFluidized Bed Dryer (VFBD). The aim of the present work was to optimize the best operating conditions for the drying of Matricaria recutita flower in the VFBD based on experimental design techniques. Response Surface Methodology (RSM) and Central Composite Design (CCD) based on 4-variable with 5-level have been employed to achieve the desirable possible combinations of frequency of vibration (7-15 Hz), inlet air temperature (36-68 °C), air flow rate (16-24 m^3/h), and drying time (30-70 min) for the highest responses in terms of moisture removal (MR) and thermal efficiency (η). A full quadratic model was used to describe the effects of individual and interactive parameters on the responses. The analysis of the obtained results showed that the inlet air temperature has the largest effect on responses. The optimal process parameters were as follows: frequency of vibration of 10.88 Hz, inlet air temperature of 64.08 °C, air flow rate of 20.63 m^3/h and drying time of 69.11 min in which the predicted value for the MR (%) and η (%) was 86.76 and 53.05, respectively. The proposed optimal conditions were examined in the laboratory and MR (%) and η (%) achieved as 87.12±0.25% and 52.78±0.34%, respectively. The experimental values agreed with those predicted by RSM models, thus indicating the suitability of the model employed and the success of RSM in optimizing the drying conditions.*

KEYWORDS: *Matricaria recutita flower; Response surface methodology; Vibrofluidized bed dryer; Moisture removal; Thermal efficiency.*

INTRODUCTION

Matricaria recutita (family of asteraceae) is one of the most popular medicinal plants that extensively consumed as a tea or tisanes around the world. Traditionally aerial parts of this plant, especially its flowers, are used for the treatment of many ailments such as allergy disorders and inflammatory mediated diseases [1].

***** *To whom correspondence should be addressed.*
+ E-mail: mrrahimi@yu.ac.ir
1021-9986/2018/4/221-233 13/$/6.03

Drying of herbs inhibits certain biochemical changes and prevents microbial growth [2, 3]. Furthermore, the drying of materials causes a substantial reduction in volume and weight, minimizing packaging, storage, and transportation costs [4]. Several different techniques include freeze drying [5], hot air drying [6, 7], natural drying [8], vibrofluidized bed dryer [9], packed and fluidized bbed [10] and Infrared Radiation (IR) drying [4] have been employed for dehydration of medicinal herbs. Among them, natural drying and hot air drying widely used because of their lower cost [11]. However, these methods have several drawbacks such as the inability to handle the large quantities and to achieve consistent quality standards, the low energy efficiency and long drying time [12]. Hence, a suitable drying technique is an important factor to enhance the quality of the dried medicinal plants. Furthermore, intensified drying techniques have more benefits. So, a suitable drying technique for medicinal plants should have some important characteristics such as Reduction in drying time (shortening the production time), uniform quality, high thermal efficiency, low cost, and operability.

Fluidized bed drying has been proposed as an alternative technique in the drying of different substances. VibroFluidized Bed (VFB) is certainly an emerging technique in the food industry since it is reported that many advantages such as reduction of minimum fluidization velocity, intensification of heat and mass transfer rate, reduction of attrition and feasibility to obtain excellent conditions of heat and mass transfer compared to conventional fluidized beds [13, 14]. Although many publications can be found the drying of various materials in fluidized beds of different kinds [9,15], such publication regarding drying of medicinal plants is rare. To the best knowledge of authors, no publication was found before the first effort by authors, regarding the effect of drying method on the chemical composition of essential oil of *Myrtus communis* L. leaves [16]. It was shown that vibro-spouted bed drying is a suitable method of drying for this plant. Intensification of heat and mass transfer rates is a well-known mean to enhance the drying rate. Also avoiding the agglomeration of wet materials is another important factor to enhance the drying and keep uniform quality dried materials. Considering above mentioned factors, a suitable technique for drying of medicinal plants is suggested and investigated experimentally. As a part of background studies concentrated on the intensification of medicinal plant drying, this study is focused on the optimization of operating conditions using experimental design techniques.

Several affecting variables such as frequency of vibration, inlet air temperature, air flow rate and drying time on VFBD performance was investigated and optimized. It is to be noted that the determining suitable operating variables is very important and also studying the interactive effect of various variables need to apply methods to be able for simultaneous optimization while considering the interaction of variables. Response Surface Methodology (RSM) is a useful model for optimizing different complex processes. Several authors have applied this technique as a collection of a statistical and mathematical system that has been successfully used to optimized drying process [6, 17-20]. *Muzaffar et al.* [21] optimize the process factors for construction of spray dried tamarind pulp powder using Response Surface Methodology (RSM). The independent variables were Soya Protein Isolate (SPI) concentration, inlet air temperature, and feed flow rate. The results exhibited that the most desirable optimum spray drying conditions for the development of tamarind pulp powder with optimum quality were 25% SPI concentration, 170 °C inlet temperature and 400 mL/h feed flow rate. Response surface methodology and synthetic evaluation method applied to optimize the drying process of okara in an Air Jet Impingement Drier (AJID) by *Wang et al.* [22]. Air temperature, air velocity, and sample loading density were considered as treatment factors in the optimization, while drying rate, color, trypsin inhibitor activity, soy isoflavone content and antioxidant activity were evaluated as responding quality parameters. The optimum conditions for AJID of okara were identified as 70°C, 2.3 m/s air velocity, and 3 kg/m^2 loading density.

In this study, the main objective was to investigate the performance of the VFB for drying of *Matricaria recutita* flowers. The influence of different factors such as: frequency of vibration, inlet air temperature, air flow rate and drying time on the MR (%) and η(%) were studied using RSM, applying a CCD (4 factors and 5 levels).

EXPERIMENTAL SECTION

Plant material

The flowers of *Matricaria recutita* L. were collected from the region of Norabad city (29º33′N, 30º1′E) (Fars province, Iran). The collected samples stored

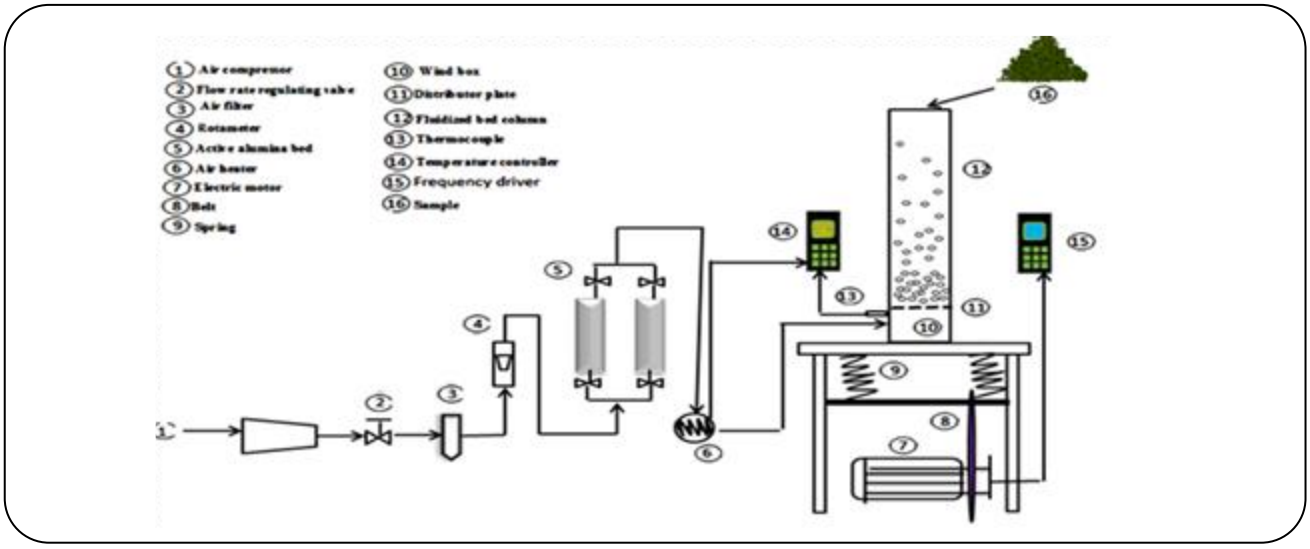

Fig. 1: Schematic diagram of the experimental apparatus.

at a temperature of 4 °C until drying experiments to preserve their original quality.

Drying equipment and experimental procedure

Drying experiments were conducted at the Process Intensification Research Lab; Department of Chemical Engineering, Yasouj University, Iran. The Schematic diagram of the experimental setup is illustrated in Fig. 1. The major components of rig are acrylic tube, oil filter, air flow meter, electrical motor, temperature controller, air heater and vibration generation system. The cylindrical vibrofluidized bed column (12) is made of acrylic which was 0.80 m high with an internal diameter of 0.10 m. This column was separated from a 0.20 m high windbox (10) which serves to improve the air distribution in the bed. A sieve plate (11) is used as a gas distributor made from stainless steel of 2 mm thickness, which arranged in a triangular pattern.

Air supply, provided by compressor draw from ambient (1) is adjusted by a ball valve (2). Before entering the acrylic tube, the air passed through a filter system (3) for the retention of probable oil and dust. The gas flow rate was measured and controlled by calibrated rotameter (4), after which a fixed bed of active alumina (5) was used for removing input air humidity and consequently through the heater (6) which contained of heating elements controlled by a rheostat to increase air temperature. The vibration system consists of an electrical motor (7) where was controlled by means of a belt (8) and springs (9). The vibration frequency can be adjusted precisely by a variable frequency driver (15). The vibration was applied in the vertical direction. The air temperature was measured by a PT-100 thermocouple (13) and controlled by a Proportional, Integral and Derivative (PID) controller (14) (Autonics, Korea). The temperature and percentage relative humidity of the exiting air were measured to an accuracy of ±5% using an electronic humidity/temperature meter (Model Lurton LM-81-HT, Taiwan).

Dehydration conditions, such as frequency of vibration (X_1:7-15 Hz), inlet air temperature (X_2:36-68ºC), air flow rate (X_3:16-24 m^3/h), and drying time (X_4:30-70 min) were selected as the effective factors on the drying procedure. The weight of the samples was measured by using an electronic balance with a precision of 1 mg (Sartorius, BP610, Germany). In all experiments, 150-g samples (16) of *Matricaria recutita* flowers which were charged in to the bed through the opening at the top of the column. In each experiment, the system was run for 30 min to achieve steady state conditions of drying before introducing drying material.

Determination of final moisture content

The Moisture Content (MC) was determined using a moisture analyzer (Sartorius MA 35, Germany). To determine the final moisture of each sample, two grams of the sample was put on inside of an aluminum pan (in the analyzer) at a temperature of 105ºC for 30 min.

The initial MC of fresh *Matricaria recutita* flower was (81.34±0.7) %. The MC of dried samples was expressed in percentage on a wet basis.

Determination of moisture removal (MR) and thermal efficiency (η)

In order to achieve the optimized drying conditions, the percentage of MR and η were chosen as the responses for the design experiment. The calculated MR (%) is defined as the following equation:

$$MR(\%) = \frac{MC_i - MC_f}{MC_i} \times 100 \quad (1)$$

Where MR is the percentage of moisture removal (%), MC_i is the initial moisture content and MC_f is the final moisture content.

The performance of VFBD was evaluated by determination of the thermal efficiency (η). The thermal efficiency (η) of the dryer was measured in terms of the inlet (T_{gi}) and the outlet (T_{ge}) drying gas temperature and the temperature of the surrounding environment (T_{amb}) and is expressed according to the following equation [23]:

$$\eta(\%) = \frac{T_{gi} - T_{ge}}{T_{gi} - T_{amb}} \times 100 \quad (2)$$

Experimental design

The drying parameters were optimized by RSM. Experiments were conducted according to CCD (Table1). Operating conditions such as frequency of vibration (X_1, Hz), inlet air temperature (X_2, ºC), air flow rate (X_3, m^3/h) and drying time (X_4, min) were chosen as independent variables for optimization on the MR (%) and η(%) as the responses (dependent variables).

The total number of design points required (N) is determined by the following equation [24]:

$$N = 2^f + 2f + N_0 \quad (3)$$

Where f is the number of variables, 2^f is the number of factorial points, 2f is the number of axial points (star point), and N_0 is the number center points. Accordingly, a design layout completely 31trials (including 16 factorial points, 8 axial points, 7 replicates at the center points) was used for the CCD. Each variable was approved into five levels (+2, +1, 0, −1, −2) and range of factor levels and the design matrix with the respect responses are listed in Table 1.

Experimental data were fitted by a second-order polynomial model and is expressed by the following equation:

$$Y_i = \beta_0 + \sum_{i=1}^{k} \beta_i X_i + \sum_{i=1}^{k} \beta_{ii} X_i^2 + \sum_{i=1}^{k} \sum_{j=i+1}^{k} \beta_{ij} X_{ij} \quad (4)$$

Where Y_i is the predicted response, which is calculated by the model, X_i and X_j are independent variables; k is the number of independent variables, β_0 is the intercept, β_i is the ith linear coefficient, β_{ii} is the ith quadratic coefficient and β_{ij} is the ijth interaction coefficient.

Statistical analysis

The Design-Expert software, version 7.0 (Stat-Ease Inc., Minneapolis, MN, USA) was applied for data analysis and optimization procedure. Statistical analysis of the model was performed to assess the analysis of variance (ANOVA). The quality of the polynomial model equation was evaluated by Lack of Fit (LOF), F-value and the determination of coefficient R^2. P-values less than 0.05 were considered to be statistically significant.

RESULTS AND DISCUSSION

Analysis of variance

The CCD was carried out to determine the model equation to predict the effects of process parameters on MR (%) and η (%). Through multiple regression analysis on the experimental data, the model for the predicted responses could be expressed by the following quadratic polynomial equation (in the form of coded values) for MR (%) and η(%), respectively:

$$MR(\%) = 75.53 + 5.17X_1 + 11.62X_2 + 3.30X_3 + 4.18X_4 - 1.89X_1^2 - 3.81X_2^2 - 2.35X_3^2 - 1.28X_4^2 - 2.77X_1X_2 + 1.15X_1X_3 - 0.76X_1X_4 - 1.47X_2X_3 - 0.35X_2X_4 - 0.73X_3X_4 \quad (5)$$

$$\eta(\%) = 43.56 + 3.13X_1 + 7.02X_2 + 1.88X_3 + 2.85X_4 - 0.78X_1^2 - 1.83X_2^2 - 1.20X_3^2 - 0.36X_4^2 - 1.42X_1X_2 + 0.37X_1X_3 - 0.67X_1X_4 - 0.47X_2X_3 - 0.46X_2X_4 - 0.0063X_3X_4 \quad (6)$$

Table 1: Central composite design for four independent variables used in this study along with the observed responses.

Factors	Levels			Star point α= 2	
	Low(−1)	Central(0)	High(+1)	-α	+α
(X_1) Vibration frequency (Hz)	9	11	13	7	15
(X_2) Inlet air temperature (ºC)	44	52	60	36	68
(X_3)Air flow rate ($m^3\ h^{-1}$)	18	20	22	16	24
(X_4) Drying time (min)	40	50	60	30	70

Runs	(X_1)	(X_2)	(X_3)	(X_4)	MR (%)	η (%)
1	1	1	-1	1	79.75	46.2
2	1	-1	-1	1	59.48	37.5
3	0	0	0	0	76.13	45.9
4	0	0	2	0	72.25	41.1
5	0	0	0	2	79.20	47.8
6	0	2	0	0	84.12	52.8
7	-1	-1	-1	-1	35.25	18.4
8	-1	1	1	-1	70.93	40.3
9	-1	-1	-1	1	48.01	29.8
10	0	0	0	0	76.72	44.2
11	0	0	0	0	76.13	43.7
12	1	1	-1	-1	74.46	42.5
13	0	0	0	0	76.12	45.1
14	2	0	0	0	78.95	47.3
15	-1	-1	1	1	53.49	34.1
16	1	1	1	1	86.98	53.3
17	0	0	-2	0	62.76	39.1
18	-1	1	1	1	81.12	49.2
19	1	1	1	-1	79.42	47.2
20	0	0	0	0	74.29	41.9
21	-2	0	0	0	59.71	36.3
22	0	0	0	0	73.12	41.6
23	0	-2	0	0	39.23	22.1
24	0	0	0	-2	64.34	39.1
25	1	-1	1	-1	63.78	38.2
26	-1	1	-1	1	78.75	43.8
27	0	0	0	0	76.23	42.5
28	1	-1	1	1	72.87	41.1
29	-1	-1	1	-1	45.56	26.7
30	1	-1	-1	-1	51.12	30.2
31	-1	1	-1	-1	68.22	40.8

In the present work, analysis of variance (ANOVA) Table 2 shows that the F-value for MR (%) and η(%) were 101.54 and 21.83.

It can be concluded that the model obtained from Eqs. (5) and (6) was significant at 95% confidence level. In addition, the fitness of the model was evaluated by the determination of coefficient (R^2), which was found to be 0.9889 and 0.9503 for MR (%) and η(%), respectively. This finding indicated that 98.89% and 95.03% of the variations could be explained by the fitted models. Normally, a regression model with $R^2 > 0.90$ is considered to have a very high correlation [25].

It is important to notice that in a suitable statistical model, the adjusted determination coefficient (R^2_{adj}) should be close to R^2 [26]. As presented in Table 2, R^2_{adj} were 0.9791 and 0.9067 for MR (%) and η (%) respectively, which indicated a high degree of correlation between the observed and predicted values.

The Lack of Fit (LOF) is a special analytical test shows the selected models are suitable reliability to explain the experimental data, or whether another model should be used. As presented in Table 2, the F-values and p-values for MR (%) and η (%) were (2.89, 3.08) and (0.1032, 0.0904) respectively, implied that the LOF was insignificant relative to the pure error. Therefore, the models fit were acceptable to describe the experimental data [27, 28].

Adequate precision measures the signal to noise ratio. According to other studies the models precision is adequate if adequate precision values >4.0 [24, 25]. In the present study, the values of models Adequate precision were 36.454 and 17.259 for MR (%) and η (%), respectively. These could be used to navigate the design space. The Coefficient of the Variation (CV) values were 2.84 for MR (%) and 6.14 for η(%), which indicates a better precision and reliability of the experimental values.

As shown in table 2, the P-values were used as a tool to check the significance of each coefficient following analysis of variance (ANOVA). According to previous studies, the corresponding coefficient with lower p-value and greater F-value represents more significant into this model [26]. The regression coefficients and the corresponding P-values were also presented in Table 2. It can be seen from this table that the linear coefficients (X_1, X_2, X_3, X_4), a quadratic term coefficient (X_1^2, X_2^2, X_3^2, X_4^2) and cross product coefficients (X_1X_2, X_1X_3, X_2X_3) were significant ($P<0.01$) for MR(%). The other term coefficients were not significant ($p>0.05$). Meanwhile, for η(%), the linear coefficients (X_1, X_2, X_3, X_4), a quadratic term coefficient (X_2^2, X_3^2) and cross product coefficients (X_1X_2) were significant.

Moreover, ANOVA (Table 2) elucidates the model insignificant terms ($p > 0.05$). Thus the final modified models for MR (%) and η (%) in terms of coded factors are:

$$MR(\%) = 75.53 + 5.17X_1 + 11.62X_2 + 3.30X_3 + 4.18X_4 - 1.89X_1^2 - 3.81X_2^2 - 2.35X_3^2 - 1.28X_4^2 - 2.77X_1X_2 + 1.15X_1X_3 - 1.47X_2X_3 \quad (5)$$

$$\eta(\%) = 43.56 + 3.13X_1 + 7.02X_2 + 1.88X_3 + 2.85X_4 - 1.83X_2^2 - 1.20X_3^2 - 1.42X_1X_2 1.42X_1X_2 + 0.37X_1X_3 - 0.67X_1X_4 - 0.47X_2X_3 - \quad (6)$$

It is obvious from Eq. (7) as well as from ANOVA (Table 2) that X_2 (F-value 863.33) is the most noticeable factor followed by X_1, X_3, and X_4 influencing MR (%). Similar results reported on the positive effect of inlet air temperature in the enhancement of the overall drying rate. In general, it was concluded that the higher vapor pressure of water corresponding to higher material temperature, which results in enhanced mass transfer driving force [20].

In the case of η (%), Table 2 shows that the X_2 was the most significant factor, followed by X_1, X_3, and X_4. The influence on the η (%) decreased in the following order: inlet air temperature >frequency of vibration>drying time> air flow rate.

Indeed, it is important to check the fitted model to confirm that it provides an adequate approximation to the real system. The plots of the predicted values vs. the observed response is shown in Figs. 2a and 2b for MR(%) and η(%), respectively. It was found that the response values predicted by the models were close to those obtained from experimental data (Fig. 2).

Response surface plot analysis

Usually, the fitted polynomial equation is expressed as surface and contour plots to visualize the relationship between the response and experimental levels of each

Table 2: Regression equation coefficients for selected responses.

Factors	MR (%)					η(%)		
	Coefficients	Sumof square	F-value	P-value	Coefficients	Sum of square	F-value	P-value
Model	75.53	5334.87	101.54	< 0.0001	43.56	1877.02	21.83	< 0.0001
X_1	5.17	640.77	170.74	< 0.0001	3.13	235.00	38.27	< 0.0001
X_2	11.62	3239.89	863.33	< 0.0001	7.02	1183.01	192.66	< 0.0001
X_3	3.30	260.63	69.45	< 0.0001	1.88	84.75	13.80	0.0019
X_4	4.18	420.26	111.99	< 0.0001	2.85	194.37	31.65	< 0.0001
X_1^2	–1.89	122.93	27.34	< 0.0001	–0.78	17.21	2.80	0.1136
X_2^2	–3.81	21.09	110.49	< 0.0001	–1.83	95.32	15.52	0.0012
X_3^2	–2.35	9.17	42.09	< 0.0001	–1.20	41.23	6.71	0.0197
X_4^2	–1.28	34.72	12.56	0.0027	–0.36	3.77	0.61	0.4446
X_1X_2	–2.77	1.94	32.76	< 0.0001	–1.42	32.21	5.24	0.0359
X_1X_3	1.15	0.086	5.62	0.0307	0.37	2.18	0.35	0.56
X_1X_4	–0.76	102.59	2.44	0.1377	–0.67	7.16	1.17	0.2964
X_2X_3	–1.47	414.63	9.25	0.0077	–0.47	3.52	0.57	0.4602
X_2X_4	–0.35	157.97	0.52	0.4826	–0.46	3.33	0.54	0.4721
X_3X_4	–0.073	47.15	0.023	0.8819	0.0063	0.0006	0.0001	0.9921
Residual		60.04				98.25		
Lack of Fit		49.73	2.89	0.1032		82.25	3.08	0.0904
Pure Error		10.32				16.00		
Cor Total		5394.91				1975.27		
R^2		0.9889				0.9503		
Adj. R^2		0.9791				0.9067		
Adequate Precision		36.454				17.259		
C.V %		2.84				6.14		

factor and to realize the optimum conditions [31, 32]. These types of plots are generated through the effects of two factors on the response at a time while the other variables are fixed at central levels. The shapes of the contour plots, circular or elliptical, are important to understand whether mutual interactions between the variables are significant or not. The circular contour plot shows that the interactions between the corresponding variables are trivial, whereas the elliptical contour plot indicates that the interactions between the corresponding variables are significant [33, 34]

Moisture Removal (MR)

The graphic representation of mutual interaction between the corresponding variables for MR (%) was shown in Figs. 3 and 4. It is interesting to note that all the contour plots in Fig. 4 were elliptical indicating the significant interaction effects between the parameters studied.

The 3-D response surface plot and the contour plot in Figs. 3a and 4a, which give the MR (%) as a function of the frequency of vibration (X_1) and inlet air temperature (X_2). It indicates that the MR (%) increase with the increasing

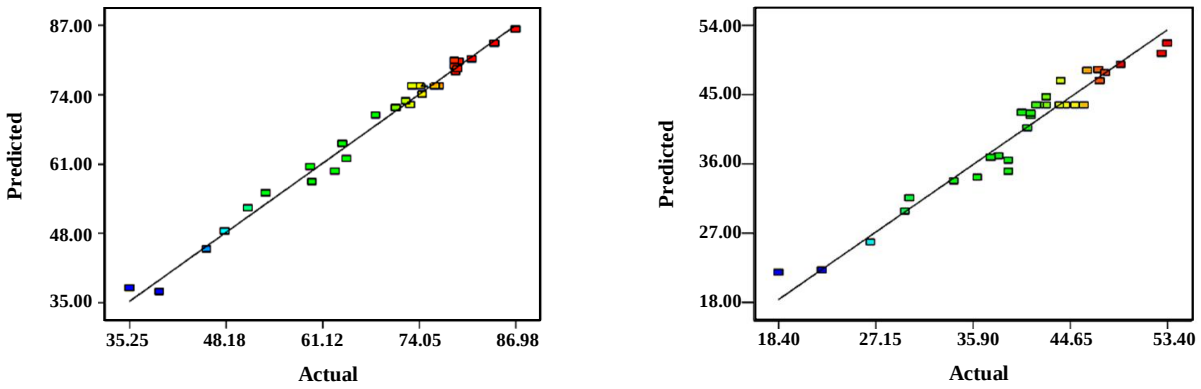

Fig.2: Plot of residuals versus predicted values for modeled responses: (a) MR (%), (b) η(%).

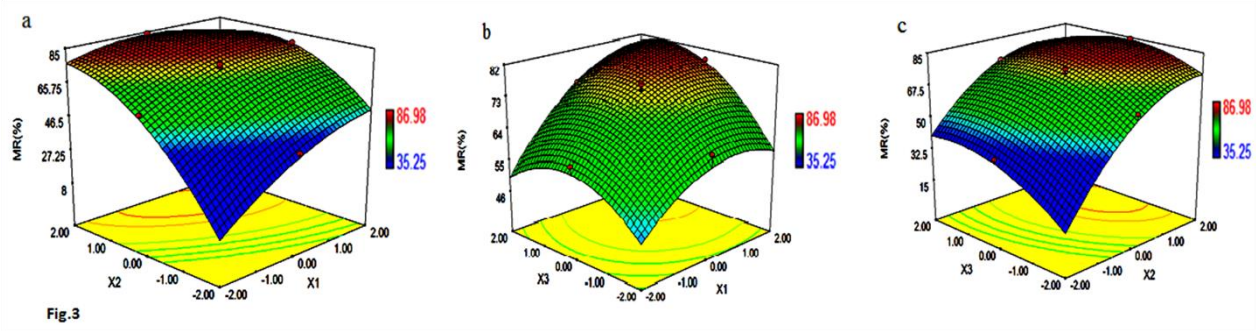

Fig. 3: Response surface plot of the combined (a) vibration frequency (X1) and inlet air temperature (X2); (b) vibration frequency (X1) and air flow rate (X3); (c) inlet air temperature (X2) and air flow rate (X3).

of the frequency of vibration. It observes that the MR (%) increase with the increasing inlet air temperature from 36 to 64.7 ◦C, meaning that further increases in inlet air temperature cannot increase the MR (%). Moreover, the elliptical contour plots in Fig. 4a show that there is a significant interaction between the indicated variables. It was observed that the percentage of MR increased with increasing the frequency of vibration and inlet air temperature. As the frequency of vibration increased, intensify heat transfer between the bed material and gas. Generally, the influence of vibrations on process intensification drying is s attributed to an increased value of the transfer coefficients by increased turbulence in the boundary layer. Also, an increase in the interfacial area as a result of the vibration reaction on the bed structure. Also, when the inlet air temperature is increased, the drying rate increases too.

The combined effects of frequency of vibration (X_1) and air flow rate (X_3) on the response are illustrated in Figs. 3b and 4b. From Fig. 3b, both frequencies of vibration and air flow rate have a quadratic effect on response. MR (%) increased at first and then decreased quickly with the increase of the two indicated factors. The maximum MR (%) is achieved when the frequency of vibration and air flow rate are 11.2 Hz and 21.1 m^3/h, respectively. It reveals that the mutual interactions between these two factors are significant due to the elliptical contour plots (Fig. 4b), which is also confirmed by the results in Table 2. An increase in the drying rate with an increase in air flow rate is attributed to the reduction in external mass transfer resistance.

The effects of the inlet air temperature (X_2) and air flow rate (X_3) on the MR (%) could be seen in Figs. 3c and 4c. The response significantly increased with the increase of the inlet air temperature from 36 to 63.4◦C, then did not further increase with increasing inlet air temperature and reached the maximum value when air flow rate at 21.8 m^3/h, and beyond this level, MR (%)

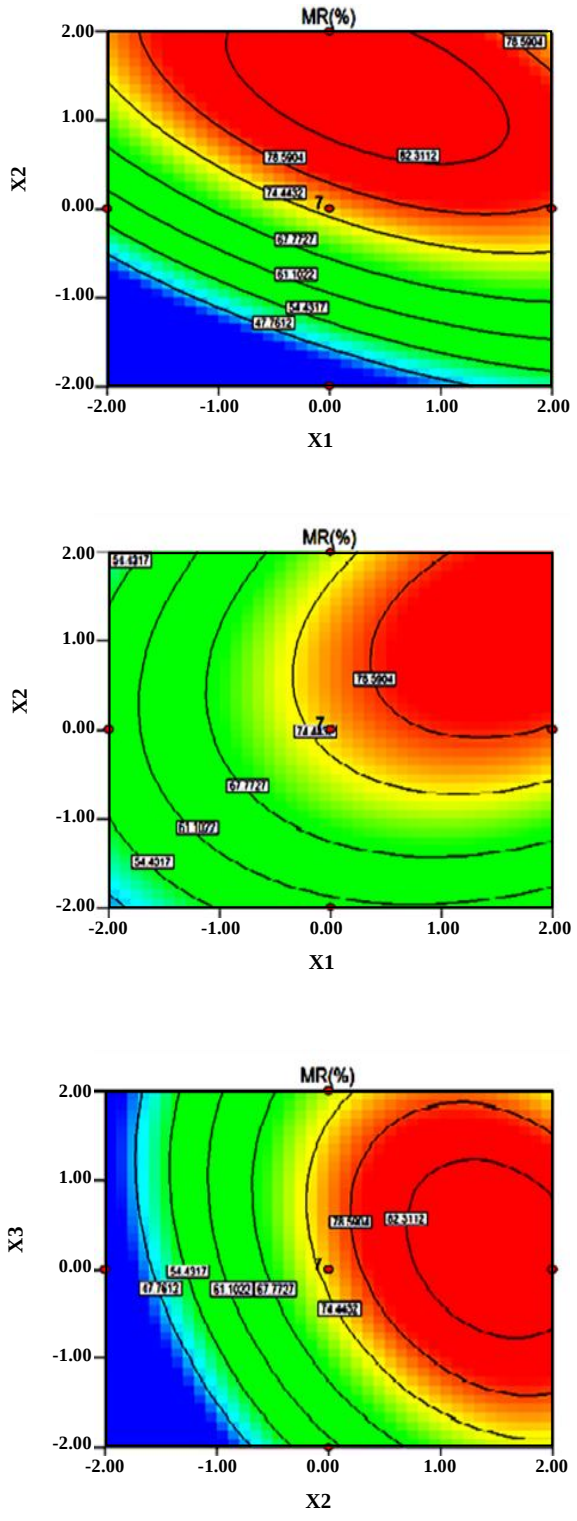

Fig. 4: Contour plot of the combined (a) vibration frequency (X1) and inlet air temperature (X2); (b) vibration frequency (X1) and air flow rate (X3); (c) inlet air temperature (X2) and air flow rate (X3).

did not further increase. Moreover, the mutual interactions between inlet air temperature and air flow rate were also significant.

Thermal efficiency (η)

Process variables were optimized for a maximum value of η (%). Surface plot and contour plot of η (%) which are presented in Fig. 5 showed that there was an interaction between the frequency of vibration (X_1) and inlet air temperature (X_2). Meanwhile, the interaction between other factors was not significant, confirming the results given in Table 2.

Figs. 5a and 5b present the 3-D response surface plot and the contour plot at a varying frequency of vibration (X_1) and inlet air temperature (X_2) on the η (%). From two figures, we can conclude that the η (%) increases when the frequency of vibration and inlet air temperature increase in the range of 7–11.2 Hz and 30–62.4 ◦C, respectively; but beyond 11.2 Hz and 62.4 ◦C, η (%) decreases slightly.

OPTIMIZATION

The final objective of response surface methodology is process optimization. Therefore, the optimum condition was predicted using the numerical optimization tool of the Design Expert 7.0.0 software. The results of optimization by ramp desirability approach for maximization of MR (%) and η(%) were given in Fig. 6. According to this Fig, the suitability of the model equations for predicting optimum response values was tested under the conditions: frequency of vibration of 10.88 Hz, inlet air temperature of 64.08 ◦C, the air flow rate of 20.63 m^3/h, and drying time of 69.11 min. Under the above conditions, the predicted MR (%) and η(%) was 86.76% and 53.05 %, respectively. However, considering the operability in actual production, the optimal conditions could be modified as follows: frequency of vibration of 10.9 Hz, inlet air temperature of 64.10 ◦C, the air flow rate of 21 m^3h^{-1}, and drying time of 69 min, respectively. Under these modified conditions, the proposed optimal conditions were examined in the laboratory and MR (%) and η(%) achieved as 87.12±0.25% (N=3) and 52.78±0.34% (N=3), respectively. According to results, the experimental values agreed with those predicted by RSM models,

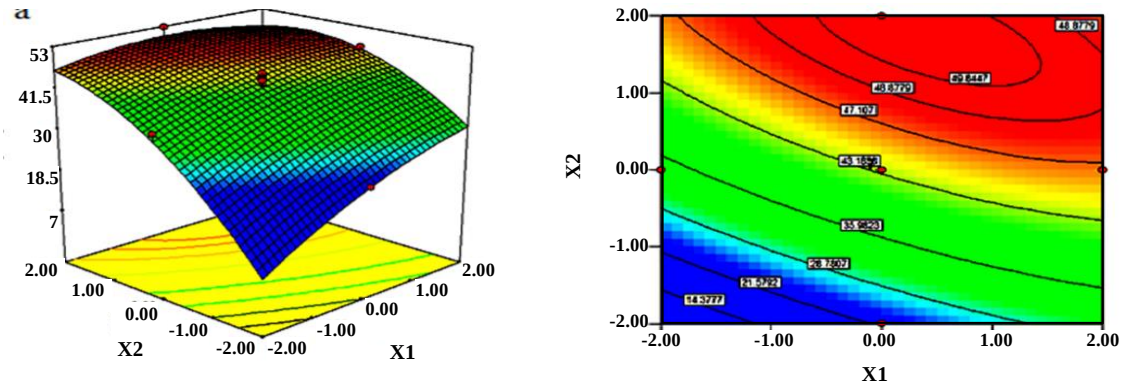

Fig. 5: (a) Response surface and (b) contour plots of the η (%) as a function of vibration frequency (X1) and inlet air temperature (X2).

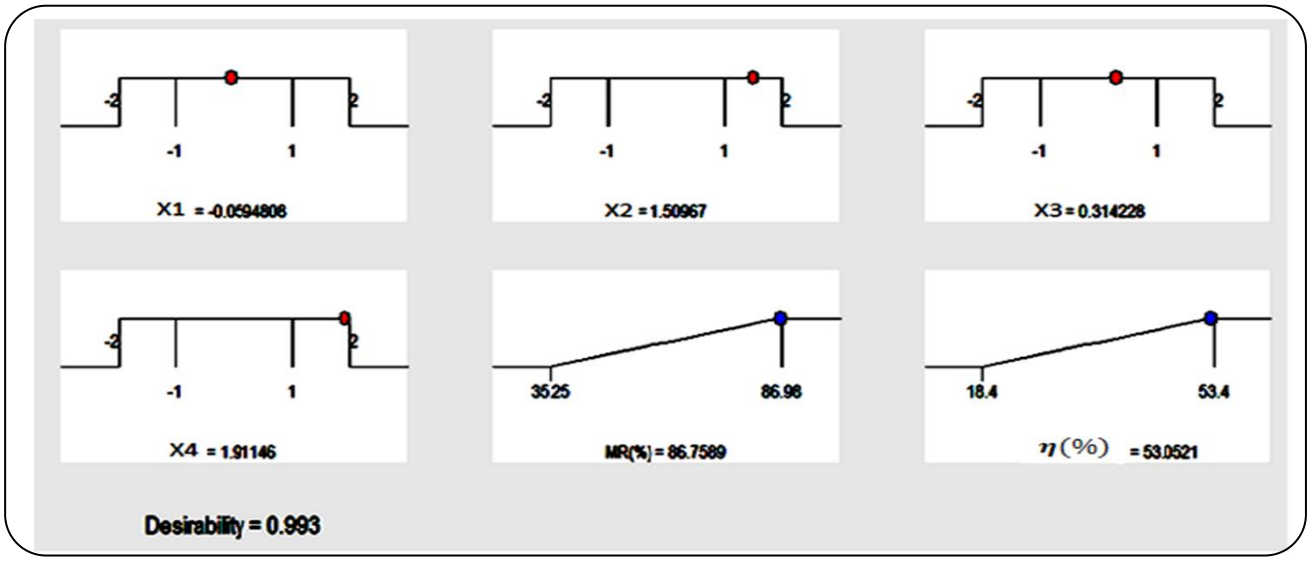

Fig. 6: Desirability ramp for numerical optimization of MR (%) and η (%).

thus indicating the suitability of the model employed and the success of RSM in optimizing the drying conditions. The optimized results for modeled responses are summarized in Table 3.

CONCLUSIONS

In this study, *Matricaria recutita* flowers were dried using a vibro fluidized bed dryer, and response surface methodology design was employed to optimize the process variables, including frequency of vibration (X_1), inlet air temperature (X_2), air flow rate (X_3) and drying time (X_4) on the responses of MR (%) and η(%). According to results, all of the four independent variables exhibited significantly quadratic effect, and cross product coefficients (X_1X_2, X_1X_3, X_2X_3) were significant on the MR (%). Meanwhile, for η (%), the quadratic term coefficient (X_2^2, X_3^2) and cross product coefficients (X_1X_2) were significant.

Also, the optimized conditions are as follows: frequency of vibration of 10.9 Hz, inlet air temperature of 64.1 ◦C, the air flow rate of 21 m^3/h and drying time of 69 min. Under this condition, the mean experimental value of MR (%) and η(%) were 87.12±0.25 and 52.78±0.34 respectively. According to results, the experimental values agreed with those predicted by RSM models, thus indicating the suitability of the model employed and the success of RSM in optimizing the drying conditions.

Table 3: Comparison between predicted and observed responses at the optimum condition obtained from RSM.

Factors name	Coded factors	Factors values	MR (%)		η (%)	
			Pred.	Exper.	Pred.	Exper.
Vibration frequency	–0.0694808	10.88 (Hz)	86.7689	87.12±0.25[a]	53.0521	52.78±0.34[a]
Inlet air temperature	1.50967	64.08(◦C)				
Air flow rate	0.31422	20.63(m^3 h^{-1})				
Drying time	1.91146	69.11(min)				

Symbols used

X_1	Frequency of vibration, Hz
X_2	Inlet air temperatures, °C
X_3	Air flow rate, m^3/h
X_4	Drying time, min
T_{gi}	Inlet drying gas temperature, °C
T_{ge}	Outlet drying gas temperature, °C
T_{amb}	The temperature of the surrounding environment, °C
Y_i	Predicted response, %

Subscripts

i	Initial
f	Final

Greek letters

η	Thermal efficiency, %
β_0	Intercept
β_i	Ith linear coefficient
β_{ii}	Ith quadratic coefficient
β_{ij}	Ijth interaction coefficient

Abbreviation

VFBD	Vibro Fluidized Bed Dryer
RSM	Response Surface Methodology
CCD	Central Composite Design
MR	Moisture Removal
IR	Infrared radiation
FBD	Fluidized bed dryer
VFB	Vibrofluidized bed
SB	Spouted bed
PID	Proportional, integral and derivative
MC	Moisture content
ANOVA	Analysis of variance
LOF	Lack of fit
R^2	Determination of coefficient
R^2_{adj}	Adjusted determination of coefficient

Received : Jul. 13, 2016 ; Accepted : Oct. 16, 2017

REFERENCES

[1] Chandrashekhar V.M., Halagali K.S.R., Nidavani B., Shalavadi M.H., Biradar B.S., Biswas D., Muchchandi I.S., Anti-Allergic Activity of German Chamomile (Matricaria recutita L.) in Mast Cell Mediated Allergy Model, *J. Ethnopharmacol*, **137**(1): 336–340 (2011).

[2] Díaz-Maroto M.C., Pérez-Coello M.S., González Vinas M.A., Cabezudo M.D., Influence of Drying on the Flavor Quality of Spearmint (*Mentha spicata L.*), *J. Agric. Food. Chem*, **51**(5): 1265–1269 (2003).

[3] Hamrouni-Sellami I., Bettaieb Rebey I., Sriti J., Zohra Rahali F., Limam F., Marzouk B., Drying Sage (*Salvia officinalis L.*) Plants and Its Effects on Content, Chemical Composition, and Radical Scavenging Activity of the Essential Oil, *Food. Bioprocess. Technol*, **5**(8):2978-2989 (2011b).

[4] Hamrouni-Sellami I., Wannes W.A., Bettaieb I., Berrima S., Chahed T., Marzouk B., Limam F., Qualitative and Quantitative Changes in the Essential Oil of Laurus Nobilis L. Leaves as Affected by Different Drying Methods, *Food. Chem*, **126**(2): 691–769 (2011a).

[5] Rahimmalek M., Hossein Golib S.A., Evaluation of Six Drying Treatments with Respect to Essential oil Yield, Composition and Color Characteristics of *Thymys daenensis subsp. daenensis*. Celak Leaves, *Ind. Crop. Prod*, **42**: 613-619 (2013).

[6] Erbay Z., Icier F., Optimization of Hot Air Drying of Olive Leaves Using Response Surface Methodology, *J Food Eng*, **91**(4): 533–541(2009).

[7] Torki Harchegan M., Sadeghi M., Ghanbarian D., Moheb A., Dehydration Characteristics of Whole Lemons in a Convective Hot Air Dryer, *Iran. J. Chem. Chem. Eng. (IJCCE)*, **35**:65-73(2016).

[8] Ghasemi Pirbalouti A., Oraiec M., Pouriamehrc M., Solaymani Babadia E., Effects of Drying Methods on Qualitative and Quantitative of the Essential Oil of Bakhtiari Savory (*Satureja bachtiarica Bunge*.), *Ind. Crop. Prod*, **46**: 324–327(2013).

[9] Rahimi M.R., Zamani R., Sadeghi H., An Investigation on Drying Kinetics of Chamomile Flower in Vibrofluidized Bed Dryer, *International Journal of Chemical Engineering and Applications*, **5**(2): 190-194, (2014).

[10] Mića V., Jelena J., Goran V., Branislav S., Experimental Investigation of the Drying Kinetics of Corn in a Packed and Fluidized Bed, *Iran. J. Chem. Chem. Eng. (IJCCE)*, **34**(3):43-49(2015).

[11]Soysal Y., Microwave Characteristics of Parsley, *Biosyst Eng*, **89**(2):167–173(2004).

[12] Soysal Y., Oztekin S., Technical and Economic Performance of a Tray Dryerfor Medicinal and Aromatic Plants, *J. Agric. Eng. Res*, **79**(1): 73–79 (2001).

[13] Gupta R., Mujumdar A.S., "Aerodynamics and Thermal Characteristics of Vibrated Fluid Beds: A Review", Mujumdar AS (Hemisphere Publishing, New York, USA), 1: 141-1150 (1980).

[14] Mujumdar A.S., Erdesz K., Applications of Vibration Techniques for Drying and Agglomeration in Food Processing, *Drying. Technol.*, **6**: 255-274 (1988).

[15] Abbasyadeh A., Motevali A., Ghobadian B., Khoshtaghaza M., Minaei S., Effect of Air Velocity and Temperature on Energy and Effective Moisture Diffusivity for Russian Olive in Thin-Layer Drying, *Iran. J. Chem. Chem. Eng. (IJCCE)*, **31**(1): 75-79 (2012).

[16] Rahimi M.R., Zamani R., Sadeghi H., Rahmani Tayebi A., An Experimental Study of Different Drying Methods on the Quality and Quantity Essential Oil of *Myrtus communis* L. leaves, *J. Essent. Oil. Bear. Pl*, **18**: 1395-1405 (2014).

[17] Lopesda Cunha R., dela Cruz A.G., Menegalli F.C., Effects of Operating Conditions on the Quality of Mango Pulp Dried in a Spout Fluidized Bed, *Drying Technol*, **24**(4): 423-432 (2006).

[18] Corzo O., Barcho N., Vasquez A., Optimization of a Thin Layer Drying Process for Coroba Slices, *J. Food. Eng*, **85**: 372-380 (2008).

[19] Han Q.H., Yin L.J., Li S.J., Yang B.N., Ma J.W., Optimization of Process Parameters for Microwave Vacuum Drying of Apple Slices Using Response Surface Method, *Drying Technol.*, **28**(4): 523-532 (2010).

[20] Chakraborty R., Bera M., Mukhopadhyay P., Bhattachary P., Prediction of Optimal Conditions of Infrared Assisted Freeze-Drying of Aloe Vera (Aloe Barbadensis) Using Response Surface Methodology, *Sep. Purif. Technol.*, **80**(2): 375–384 (2011).

[21] Muzaffar K., Kumar P., Parameter Optimization for Spray Drying of Tamarind Pulp Using Response Surface Methodology, *Powder. TechnoL.*, **279**: 179–184 (2015)

[22] Wang G., Deng Y., Xu X., He X., Zhao Y., Zou Y., Liu Z., Yue J., Optimization of Air Jet Impingement Drying of Okara Using Response Surface Methodology**,** *Food. Control.*, **59**: 743-749 (2016).

[23] Goula A.M., Adamopoulos K.G., Spray Drying Performance of a Laboratory Spray Dryer for Tomato Powder Preparation, *Drying Technol.*, **21**(7): 1273–1289 (2003).

[24] Morgan E., "Chemometrics: Experimental Design", John Wiley & Sons Inc., London (1991).

[25] Kundu A., Karmakar M., Ray R., Simultaneous Production of Animal Feed Enzymes (Endoxylanase and Endoglucanase) by Penicillium Janthinellum from Waste Jute Caddies, *International Journal of Recycling of Organic Waste in Agriculture*, **13**: 1-13 (2012).

[26] Liu Y., Wei S., Liao M., Optimization of Ultrasonic Extraction of Phenolic Compounds from Euryale Ferox Seed Shells Using Response Surface Methodology, *Ind. Crop. Prod.*, **49**: 837–843 (2013).

[27] Hamsaveni D.R., Prapulla S.G., Divakar S., Response Surface Methodological Approach for the Synthesis of Isobutyl Butyrate, *Process. Biochem.*, **36**: 1103-1110 (2011).

[28] Yanga Q., Chenc H., Zhouc X., Zhangd J., Optimum Extraction of Polysaccharides from Opuntia Dillenii and Evaluation of Its Antioxidant Activities, *Carbohydr. Polym.*, **97**(2): 736–742 (2013).

[29] Ferreira S.L.C., Bruns R.E., Ferreira H.S., Matos G.D., David J.M., Brandao G.C., Silva E.G.P., Portugal L.A., Reis P.S., Souza A.S., Santos W.N.L., Box–Behnken Design: an Alternative for the Optimization of Analytical Methods, *Anal. Chim. Acta*, **597**(2): 179–186(2007).

[30] Guo X., Zou X., Sun, M., Optimization of Extraction Process by Response Surface Methodology and Preliminary Characterization of Polysaccharides from Phellinus Ignoramus, *Carbohydr. Polym.*, **80**(2): 344–349 (2010).

[31] Wei Z.J., Liao A.M., Zhang H.X., Liu J., Jiang S.T., Optimization of Supercritical Carbon Dioxide Extraction of Silkworm Pupal Oil Applying the Response Surface Methodology, *Bioresour. Technol.*, **100**(18): 4214–4219 (2009).

[32] Lu C.H., Engelmann N.J., Lila M.A., Erdman J.W., Optimization Oflycopene Extraction from Tomato Cell Suspension Culture by Response Surface Methodology, *J. Agric. Food. Chem.*, **56**(17): 7710–7714 (2008).

[33] Anuradha Jabasingh S., Valli Nachiyar C., Utilization of Pretreated Bagasse for the Sustainable Bioproduction of Cellulase by Aspergillus Nidulans MTCC344 Using Response Surface Methodology, *Ind. Crop. Prod.*, **34**(3): 1564–1571 (2011)

[34] Muralidhar R.V., Chirumamila R.R., Marchant R., Nigam P., A Response Surfaceapproach for the Comparison of Lipase Production by Candida Cylindracea Using Two Different Carbon Sources, *Biochem. Eng. J.*, **9**(1):17–23 (2001).